Publisher homepage: www.universepg.com, ISSN: 2707-4625 (Online) & 2707-4617 (Print)

https://doi.org/10.34104/ijmms.023.041051

International Journal of Material and Mathematical Sciences

Journal homepage: www.universepg.com/journal/ijmms

Magnetohydrodynamic Effects on the Flow of Nanofluids Across a Convectively Heated Inclined Plate Through a Porous Medium with a Convective Boundary Layer

E. Esekhaigbe[1]*, Uchenna A. Uka[2], and Alex Musa[3]

[1]Dept. of Mathematics and Computer Science, University of Africa, Bayelsa State, Nigeria; [2]Dept. of Basic Sciences, School of Science and Technology, Babcock University, Ogun State, Nigeria; [3]Dept. of Mathematics and Statistics, University of Port Harcourt, Rivers State, Nigeria.

*Correspondence: eskhaigbe.edwin@uat.edu.ng (E. Esekhaigbe, Department of Mathematics and Computer Science, University of Africa, Bayelsa State, Nigeria).

ABSTRACT

The study explores the problem of Magnetohydrodynamic natural convection boundary layer flow of a nanofluid past a convectively heated inclined porous channel. The governing partial differential equations have been transformed through appropriate similarity functions into nonlinear ordinary differential equations. The emerging equations were solved numerically using both a sixth-order Runge-Kutta-Fehlberg and the shooting technique. The influences of pertinent parameters such as plate inclination angle, magnetic field, buoyancy ratio, and the convective heating term on the temperature, velocity, and concentration profiles were investigated graphically. Key findings indicate that an increase in magnetic field and permeability leads to a decline in the fluid's velocity while the temperature and nanoparticle concentration are significantly enhanced. The results obtained are in close correlation with existing body of knowledge discussed in the literature.

Keywords: MHD, Maple, Nonlinear, Nanofluid, Coupled ode, Nanoparticle, and Partial differential equations.

INTRODUCTION:

The recent surge in nanofluid research has attracted scholar's interest worldwide, mostly due to its extensive applications in several industries, especially leading-edge businesses specialising in nano-devices. The utilisation of nanofluids has been extensively explored and documented in a substantial body of research, as referenced in (Goyal & Bhargara, 2014; Boungiorno, 2006; Al-Maman *et al.,* 2019; Muhamad *et al.,* 2023; Amer *et al.,* 2023; Ayub *et al.,* 2016). The rate of heat conduction and transfer in electronic equipment is very sluggish, which significantly hampers the operation of these systems. By incorporating nanoparticles such as copper (Cu) and alumina (Al) into a base fluid, the efficiency of heat transfer can be improved, resulting in optimal performance of the device. For an extensive examination of the nanofluids in various shapes and conditions, refer to the scholarly publications cited in references (Al-Maman *et al.,* 2019; Muhamad *et al.,* 2023; Amer *et al.,* 2023; Goyal & Bhargara, 2014; Kuznetsov & Nield, 2018; Aziz *et al.,* 2012; Dhanal *et al.,* 2015; Ahmed & Elsaid, 2019; Alam *et al.,* 2015). These papers provide valuable perspectives on many subjects pertaining to nanofluid research and its practical implementations. The imperative to consistently pursue enhancement in thermal conductivity is unavoidable, considering that low thermal conductivity poses a significant barrier in the advancement of energy-efficient heat transfer techniques, which are the vital in numerous applications.

Goyal and Bhargara, (2014) examined velocity slip boundary condition effect on the heat transfer flow of non-Newtonian nanofluids over a stretching sheet. According to the paper, there is a drop in heat and mass transfer rates as the slip parameter increases Dhanal *et al.* (2015). Conducted an investigation on the MHD boundary layer flow generated by the stretching and shrinking. According to the authors, viscous dissipation has a beneficial impact on heat and mass transmission, but Brownian motion has a minimal impact. The study conducted by Ali *et al.* (2021) demonstrated that as the concentration of Cu in water increases, the fluid velocity decreases, but the fluid temperature and concentration increases. This study examines the influence of a Cu-MHD hybrid nanofluid on heat transfer and flow in a permeable channel. The impacts of heat flux and viscous dissipation are taken into account, using a Newtonian base fluid. They observed that when the volume percentage grows, the velocity of the fluid increases while the temperature lowers. Additionally, the dissipation of viscosity contributes to an increase in the fluid's temperature. In a related development in Goyal and Bhargara, (2018) the boundary layer flow of a nanofluid was addressed using convective boundary conditions with magnetic effects. The Nusselt number was found to decrease when the inclination, buoyancy ratio, Brownian motion, and thermophoresis parameter rise, whereas it increases with an increased Prandtl number. References (Alam *et al.,* 2009; Ali *et al.,* 2013; Chen, 2004; Ali, 2012; Khan *et al.,* 2011) provide in-depth analysis of detail work on inclined planes, whereas references (Aziz & Khan, 2012; Aziz, 2009; Bejan, 2013; Narahari, 2013) address convective boundary problems.

The study conducted by Ghalambaz, (2014) investigated the spontaneous convection of nanofluids on a vertically oriented heated plate. It was noted that the thickness of the concentration profile is significantly smaller compared to the thickness of the temperature and velocity profiles. Additionally, it was observed that low convective heating leads to increased Brownian motion and affects the temperature profile. Conversely, Gunisetty *et al.* (2023) conducted research on the movement of nanofluid on a spinning disc, taking into account magnetic and radiative influences. Their primary discoveries the demonstrated a positive correlation between the velocity profile and the Weissenberg number, and an increase in the electric field and radiative parameter resulted in an enhancement of the magnetic field and porosity. Detailed study on porosity is contained in (Ali *et al.,* 2012; Khan *et al.,* 2011; Mohebbi *et al.,* 2020; Olanrewaju *et al.,* 2013). This study draws inspiration from the array of literature discussed above. Many researchers have extensively studied many facets of nanofluids due to its wide-ranging utilisation in the contemporary technological era, where efficient heat transmission has significant impact (Akter *et al*., 2023).

Nevertheless, despite the numerous factors taken into account by multiple authors, there has been limited focus on the study of natural convection nanofluid flow over an inclined porous plate subjected to the convective heating and influenced by a magnetic field. Essentially, this article delves into this novel concept. The mathematical modeling incorporated factors such as the uniform magnetic field, the permeability, and convective boundary conditions, among other considerations. The equations that describe the flow dynamics are derived and then converted into non-dimensional forms using suitable similarity functions. The numerical computations are performed by utilising MAPLE solver. Findings are depicted through graphs and tables, analysed and discussed intuitively

Mathematical Formulation

A two-dimensional, laminar, stable, and income-pressible flow with constant physical properties is considered. The semi-infinite plate is subjected to inclination φ along the vertical axis. The flow direction is tailored towards the horizontal axis, with a constant magnetic field B_0 in the vertical direction. It is assumed that the lower part of the plate is thermally heated by convection through a hot fluid at a temperature T_f with a heat transfer coefficient h_f. Further, the base fluid and nanoparticles are considered to be in thermal equilibrium. The schematic depiction of the formulation is thus demonstrated.

The continuity, momentum, energy, and nanoparticle concentration equations in Goyal and Bhargara, (2018) below serve as the governing equations for the flow under the aforementioned presumptions.

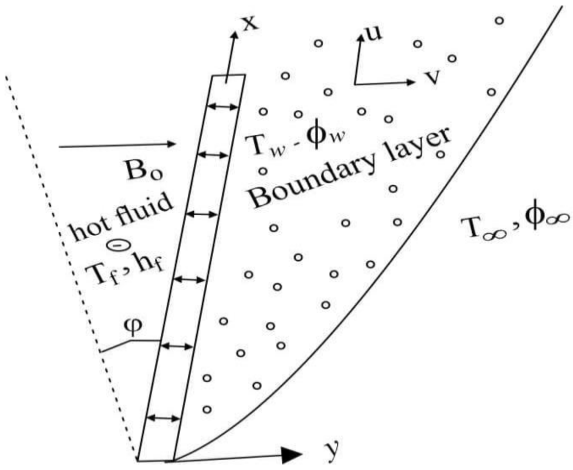

Fig. 1: Model configuration.

$$\frac{\partial u}{\partial x} + \frac{\partial v}{\partial x} = 0 \tag{1}$$

$$\rho f\left(u\frac{\partial u}{\partial x} + v\frac{\partial v}{\partial x}\right) = \mu\frac{\partial^2 u}{\partial y^2} - \sigma_n B_0^2 u - \frac{\mu}{\rho k}u + [(1-\phi_\infty)\rho f_\infty \beta g_e(T - T_\infty) - (\rho_p - \rho f_\infty)g_e(\phi - \phi_\infty))]Cos\varphi \tag{2}$$

$$u\frac{\partial T}{\partial x} + v\frac{\partial T}{\partial y} = \alpha_m \frac{\partial T^2}{\partial y^2} + \tau\left[D_B\frac{\partial \phi}{\partial y}\frac{\partial T}{\partial y} + \frac{D_T}{T_\infty}\left(\frac{\partial T}{\partial y}\right)^2\right] \tag{3}$$

$$u\frac{\partial \phi}{\partial x} + v\frac{\partial \phi}{\partial x} = D_B\frac{\partial^2 \phi}{\partial y^2} + \frac{D_T}{T_\infty}\frac{\partial^2 T}{\partial y^2} \tag{4}$$

Where u and v are the velocity components perpendicular to the plate and parallel to it, respectively; B_0 is the magnetic field; ϕ is the volume fraction of the nanoparticles; β is the thermal expansion coefficient of the base fluid; φ is the angle of inclination; D_B is the Brownian diffusion coefficient; D_T is the thermophortic diffusion coefficient; and T is the dimensional temperature. The boundary conditions we propose are;

$$u = 0,\ v = 0,\ \phi = \phi_w,\ -k\frac{\partial T}{\partial y} = h_f\left(T_f - T\right)\ at\ y = 0 \tag{5}$$

$$u = 0,\ v = 0,\ \phi = \phi_\infty,\ T = T_\infty \quad \text{as}\ y \to \infty \tag{6}$$

With $u = \partial\psi / \partial y$ and $v = -\partial\psi / \partial x$, equation (1) is identically satisfied.We deployed the similarity variables below to Equations (2)- (6);

$$\eta = \frac{y}{x}Ra_x^{\frac{1}{4}},\ \psi = \alpha_m Ra_x^{\frac{1}{4}}f(\eta),\quad \theta(\eta) = \frac{T - T_\infty}{T_f - T_\infty},\ \phi(\eta) = \frac{\phi - \phi_\infty}{\phi_f - \phi_\infty} \tag{7}$$

Where the local Rayleigh number is expressed as

$$R_{a_x} = \frac{(1-\phi_\infty)\beta g_e(T_f - T_\infty)x^3}{v_{\alpha m}} \tag{8}$$

Using Eqs. (7), and (8) in Eqs. (2)- (6), we have the equations;

$$f''' + \frac{1}{4P_r}\left(3ff'' - 2f'^2\right) + (\theta - N_r\phi)Cos\varphi - (M + K)f' = 0\quad () \tag{9}$$

$$\theta'' + \frac{3}{4} f\theta' + N_b\theta'\phi' + N_t\theta'^2 = 0 \quad (10)$$

$$\phi'' + \frac{N_t}{N_b}\theta'' + \frac{3}{4} Lef\phi' = 0 \quad (11)$$

The associated boundary conditions are transformed to the following;

$$f(\eta) = 1\,,\ f'(\eta) = 0\,,\ \ \theta'(\eta) = -NC[1-\theta(\eta)],\ \phi(\eta) = 1 \quad at\ \eta = 0 \quad (12)$$

$$f'(\eta) = 0, \theta(\eta) = 0\,, \phi(\eta) = 0\ \ as\, \eta \to \infty \quad (13)$$

In the context of equations (9) - (13), prime represent differentiation with respect to η, P_r Prandlt number, N_r Buoyancy-ratio parameter, L_e nanoparticle Lewis number N_c convective heating parameter, K the permeability parameter and M magnetic parameter. The parameters are the mathematically represented below Goyal and Bhargara, (2018).

$$P_r = \frac{\mu}{\alpha_m},\quad N_r = \frac{(\rho_p-\rho_f)(\phi_w-\phi_\infty)}{\rho_{f(1-\phi_w)}(T_f-T_\infty)},\ \ M = \frac{\sigma B_0^2 x^3}{\mu Ra_x^{\frac{1}{2}}},\ \ N_c = \frac{hx^{\frac{1}{4}}}{k}\left[\frac{v\alpha_m}{(1-\phi_\infty)g_e\beta(T-T_\infty)}\right]^{\frac{1}{4}}, K = \frac{v}{ak}$$

(14)

It is crucial to remark that the assessment of nano-fluidic device performance necessitates a thorough consideration of heat and mass transmission. Hence, it is imperative to consider two essential physical parameters pertaining to the rates of heat and mass transport, as indicated by Siddiqa *et al*. (2014). The Local Nusselt number, denoted as Nux, and the Sherwood number, denoted as Shx, is mathematically represented as follows.

$$Nu_x = \frac{xq_w}{k(T_f-T_\infty)},\ Sh_x = \frac{xj_w}{D_B(\phi_w-\phi_\infty)} \quad (15)$$

In the context of equation (15);
q_w= heat flux from the plate
j_w = mass flux from the plate
These terms are mathematically defined as;

$$q_w = -k\left(\frac{\partial T}{\partial y}\right),\ j_w = -D_B\left(\frac{\partial C}{\partial y}\right)\ \ at\ y = 0 \quad (16)$$

With equations (7) and (8), the dimensionless parameters take the form expressed in equation (17)

$$Ra_x^{\frac{1}{4}}Nu_x = -\theta'(0),\ Ra_x^{\frac{1}{4}}Sh_x = -\phi'(0) \quad (17)$$

Method of Solution

Equations (9-11), subject to Eqs. (12), and (13) were numerically treated with Maple Solver. The default numerical solution methods employed by the software for two-point boundary value problems involve the utilisation of a sixth-order Runge-Kutta Fehlberg method in conjunction with shooting techniques. The effectiveness of these strategies has been substantiated by scholarly publications Olanrewaju *et al.* (2013). A comprehensive examination of our findings is presented in the next section.

RESULTS AND DISCUSSION:

In this section, we provide graphical figures and a comprehensive discussion to the enhance the understanding of the physical aspects of this work. The obtained results are graphically shown in terms of velocity, temperature, and concentration profiles. Tables showing the computations of local Nusselt and Sherwood numbers and a diverse set of relevant parameters are shown. As seen in **Table 1**, the computed value decreases the monotonically for different values of the Prandlt number. This shows a clear correlation with the results articulated in (Bejan, 2013; Kuznetsov and Nield, 2010). In **Table 2**, the computation of *Nux* and *Shx* numbers under the influence of several pertinent parameters is presented. Results are in close correlation compare to Aziz and Khan, (2012). The dependency of the Nuselt and Sherwood numbers over variations in P_r, *Nb, and Nr* with other parameters fixed is presented. It is seen that Nusselt and Sherwood numbers increases as Pr increases whereas for fixed Pr, both decreases monotonically as *Nb* and *Nr* increases. The changes in the Magnetic field parameter, thermophoresis parameter, and the Plate's inclination angle on *Nux* and *Shx* numbers is depicted in **Table 4**. The performance of heat and transfer decreases as the plate's inclination angle and the magnetic field are steadily increased. The corresponding value of Nt are equally represented in **Table 4**. **Fig. 2**, **3**, and **4** depict the impact of the magnetic field M on the dimensionless velocity, temperature, & concentration, correspondingly. The data presented indicates a decrease in the velocity profile for increased magnetic field strength, while temperature and concentration are both enhanced. This implies that the Lorentz force, which is a type of resistive force, was generated due to the presence of a magnetic field. The force appears to impede the accumulation of momentum thereby decelerating the fluid flow and opposing the influence of M. The thermal energy is generated as a result of the increased force used during the process of pulling the nanofluid. The energy transfer leads to an increase in the temperature of the nanofluid. As a result, the presence of the magnetic field causes a reduction in the thickness of the momentum boundary layer and an augmentation in the thickness of the thermal boundary layer.

Furthermore, the phenomenon of the nanoparticle diffusion is facilitated by the warming of the boundary layer, resulting in an elevation of the concentration of the fluid, as depicted in **Fig. 4**. **Fig. 5**, **6**, and **7** depict the effect of the porosity parameter on the fluid's dimensionless velocity, temperature, and concentration profiles. Clearly, it is observed that the velocity diminishes as porosity increases. In practice, this means that higher values of porosity are indicative of increased viscous forces, which lead to a dominance of initial forces, which in turn causes the velocity to decrease. However, a gradual increase in porosity value leads to an observable enhancement in both the dimensionless temperature and concentration (see **Fig. 6** and **7**). Furthermore, the decrease in fluid velocity occasioned by an increase in porosity can be explained more by the presence of porous medium. This medium introduces obstructtions and resistance to the flow of the fluid. The medium gradually gets more obstructive as the porosity parameter rises, resulting in increased resistance, which finally causes a decrease in the fluid's velocity. In **Fig. 8**, the influence of nanofluid Lewis number on the dimensionless concentration is presented and shows a sharp decline in concentration of the nanoparticles as Le increase. Practically, for a base fluid of certain thermal diffusivity D_B, a higher *Le* indicates a lower Brownian diffusion coefficient, resulting in a shorter penetration depth for the concentration boundary layer. The word "thermophoresis" describes how particles disperse when there is a temperature gradient present. **Fig. 9** and **10** show, respectively, how the thermophoresis parameter Nt affects the dimensionless temperature and concentration. It goes without saying that altering Nt's value causes a rise in the temperature gradient and a strengthening of the force within nanoparticles. This force causes more fluid to the heat up, which likewise boosts the temperature. Enhancing the thermophoresis Nt effect yields a similar outcome for nanoparticle concentration, as shown in **Fig.10**. Due to constant collisions between nanoparticles and base fluid molecules, Brownian motion is the zigzag movement of nanoparticles inside the base fluid. **Fig. 11** and **12** demonstrate the effect of Nt on temperature and concentration. The randomness of the nanoparticles is seen to increase rapidly in a chaotic manner as Nb increases. This chaotic behaviour causes more collisions in the system. This increased collision of nanoparticles causes an increase in heat transfer properties and thus increases the temperature of the fluid. Similarly, the concentration of nanoparticles along the wall is hampered by a concurrent increase in Nb. As a result, the value of the nanoparticle concentration along the wall decreases as the nanoparticles shift from the boundary to the fluid by increasing their random motion. The impact of the convective heating parameter Nc on the velocity is examined in **Fig. 13**. A rise in Nc increases the fluid's velocity, as shown in the figure. The effects of plate inclination angle from vertical for values of $0^0, \frac{\pi}{10}, \frac{\pi}{9}$, and $\frac{\pi}{6}$ on the dimensionless velocity, temperature, and concentration are shown in **Fig. 14**, **15**, and **16**, respectively. The fluid's velocity decreases along with the boundary layer as the plate inclination angle φ is changed. The alignment of the plate is what creates the effect, through the buoyancy term in equation 2. The value of Cos φ falls in proportion as the value of φ grows. This results in the buoyancy effect disappearing as the plate's inclination angle φ increases. As a result, the driving force acting on the fluid weakens, lowering its velocity. This observation corresponds well with Alam *et al.* (2009) in terms of velocity profile. Also, **Fig. 15** and **16** clearly reflect how the depletion of the buoyancy effect enhances thermal and nanoparticle diffusion with a variation in the plate's inclination φ. **Fig. 17**, **18**, and **19** show the characteristics behaviour of the buoyancy ratio parameter on the dimensionless velocity, temperature, & concentration. As observed in the figures, while increase in the buoyancy parameter enhances the fluid's temperature and concentration, it depletes the velocity.

Table 1: Comparison of Nu_x of regular fluid for various values of Pr with $Le = 10, Nb = Nt = 10^{-5}, NC = 10, \varphi = k = 0$.

Pr	Bejan, (2013)	Kuznetsov & Nield, (2010)	Narahari, (2013)	Present Result
1	0.401	0.401	0.401	0.566
10	0.465	0.463	0.459	0.665
100	0.490	0.481	0.473	0.694
1000	0.499	0.484	0.474	0.699

Table 2: Comparison of results for Nu_x and Sh_x for $Nt = 0.1, NC = Le = 10, m = k = \varphi = 0$.

		$Pr = 1.0$				$Pr = 5.0$			
Nb	Nr	Nu_x		Sh_x		Nu_x		Sh_x	
		Aziz & Khan, (2012)	Present results	Aziz & Khan, (2012)	Present results	Aziz & Khan, (2012)	Present results	Aziz & Khan, (2012)	Present results
0.1	0.1	0.3396	0.4578	0.9954	2.0413	0.3807	0.4792	1.0608	2.1747
	0.2	0.3366	0.4571	0.9828	2.0380	0.773	0.4788	1.0482	2.1713
	0.3	0.3334	0.4564	0.9697	2.0346	0.3739	0.4785	1.0351	2.1679
	0.4	0.3301	0.4557	0.9559	2.0312	0.3702	0.4781	1.0214	2.1643
	0.5	0.3267	0.4540	0.9414	2.0271	0.3665	0.4778	1.0071	2.1608
0.3	0.1	0.2939	0.388	1.0435	2.1204	0.3306	0.4069	1.1101	2.2368
	0.2	0.2918	0.3875	1.0317	2.1176	0.3282	0.4066	1.0985	2.2339
	0.3	0.2896	0.3871	1.0195	2.1147	0.3258	0.4063	1.0866	2.2310
	0.4	0.2872	0.3867	1.0067	2.1110	0.3232	0.4061	1.0741	2.2282
	0.5	0.2848	0.3862	0.9934	2.1091	0.3206	0.4058	1.0611	2.2253
0.5	0.1	0.2530	0.3271	1.0584	2.1366	0.2855	0.3437	1.1263	2.2496
	0.2	0.2513	0.3267	1.0471	2.1334	0.2836	0.3435	1.1152	2.2469
	0.3	0.2495	0.3264	1.0353	2.1311	0.2816	0.3432	1.1037	2.2442
	0.4	0.2477	0.3261	1.0230	2.1284	0.2796	0.3431	1.0918	2.2415
	0.5	0.2458	0.3257	1.0102	2.1257	0.2775	0.3429	1.0794	2.2387

Table 3: Variations of Nu_x and Sh_x for $M, Nt\ and\ \varphi$ when $Nc = 10, Pr = 5.0, Nb = Nr = 0.5, Le = 10, K = 1.0$.

		$m = 1.0$		$m = 1.2$		$m = 1.5$	
Nt	φ	Nu_x	Sh_x	Nu_x	Sh_x	Nu_x	Sh_x
0.1	0	0.2127	1.9490	0.2095	1.9332	0.2049	1.9093
	$\frac{\pi}{10}$	0.2054	1.9232	0.2021	1.9077	0.1973	1.8856
	$\frac{\pi}{9}$	0.1986	1.9022	0.1951	1.8868	0.1902	1.8649
	$\frac{\pi}{6}$	0.1897	1.8786	0.1860	1.8634	0.1809	1.8417
0.3	0	0.1623	1.9783	0.1614	1.9602	0.1591	1.9349
	$\frac{\pi}{10}$	0.1586	1.9456	0.1570	1.9280	0.1545	1.9034
	$\frac{\pi}{9}$	0.1541	1.9192	0.1523	1.9020	0.1493	1,8779
	$\frac{\pi}{6}$	0.1477	1.8898	0.1453	1.8730	0.1419	1.8944
0.45	0	0.1226	2.0248	0.1233	2.0041	0.1236	1.9753
	$\frac{\pi}{10}$	0.1226	1.9846	0.1224	1.9648	0.1217	1.9373

	$\frac{\pi}{9}$	0.1206	1.9526	0.1198	1.9335	0.1184	1.9069
	$\frac{\pi}{6}$	0.1161	1.9173	0.1147	1,8989	0.1126	1.8731

Table 4: Variations of Nu_x and Sh_x for $Pr, Nb\ and\ Nr$ when $Nt = 0.1, \varphi = \frac{\pi}{6}, Le = 10, K = 1.0, NC = K = M = 1.0, Le = 10, K = 1.0$.

		$Pr = 1.0$		$Pr = 5.0$		$Pr = 10.0$	
Nb	Nr	Nu_x	Sh_x	Nu_x	Sh_x	Nu_x	Sh_x
0.1	0.1	0.2417	1.7657	0.2520	1.8037	0.2534	1.8088
	0.2	0.2415	1.7649	0.2518	1.8029	0.2532	1.8080
	0.3	0.2414	1.7641	0.2516	1.8021	0.2530	1.8072
	0.4	0.2412	1.7634	0.2514	1.8013	0.2528	1.8064
	0.5	0.2410	1.7626	0.2512	1.8005	0.2526	1.8056
	0.6	0.2408	1.7618	0.2511	1.7998	0.2525	1.8048
0.3	0.1	0.2104	1.8319	0.2198	1.8682	0.2211	1.8730
	0.2	0.2102	1.8312	0.2197	1.8675	0.2210	1.8723
	0.3	0.2101	1.8305	0.2196	1.8668	0.2209	1.8716
	0.4	0.21006	1.8299	0.2195	1.8662	0.2208	1.8710
	0.5	0.2099	1.8292	0.2193	1.8655	0.2201	1.8703
	0.6	0.2098	1.8285	0.2192	1.8648	0.2206	1.8696
0.5	0.1	0.1815	1.8453	0.1901	1.8813	0.1918	1.8860
	0.2	0.1814	1.8446	0.1900	1.8806	0.1913	1.8854
	0.3	0.1813	1.8440	0.1899	1.8799	0.1918	1.8847
	0.4	0.1812	1.8433	0.1898	1.8793	0.1910	1.8841
	0.5	0.1811	1.8427	0.1897	1.8786	0.1909	1.8834
	0.6	0.1811	1.8420	0.1896	1.8780	0.1908	1.8822

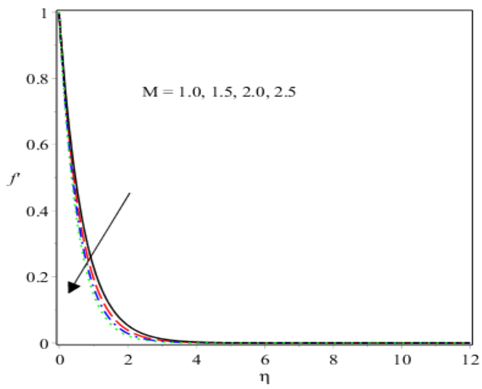

Fig. 2: Effect of *M* on velocity.

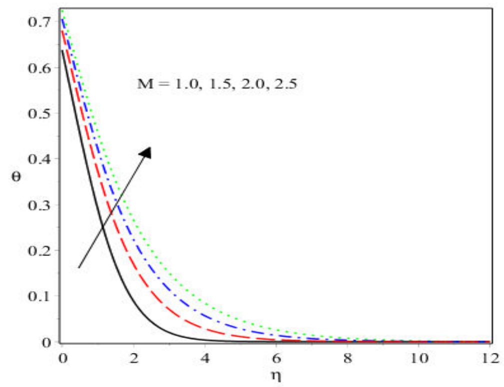

Fig. 3: Effect of *M* on temperature.

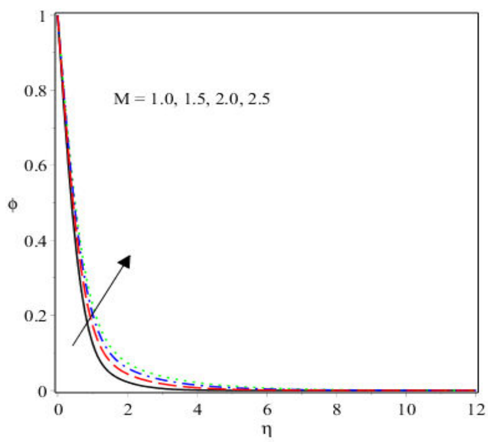

Fig. 4: Effect of *M* on concentration.

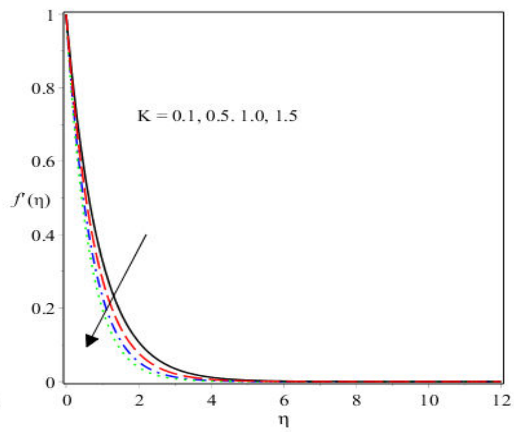

Fig. 5: Effect of *K* on velocity.

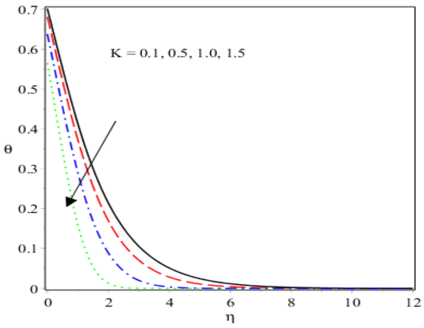

Fig. 6: Effect of *K* on temperature.

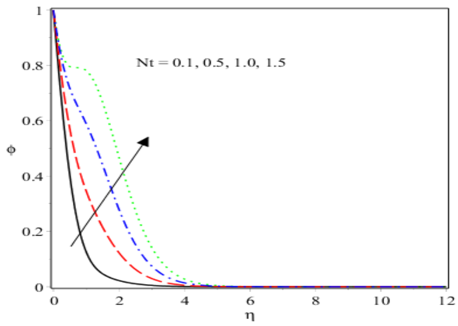

Fig. 7: Effect of *K* on concentration.

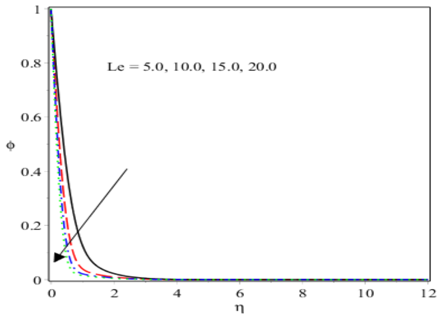

Fig. 8: Effect of *Le* on concentration.

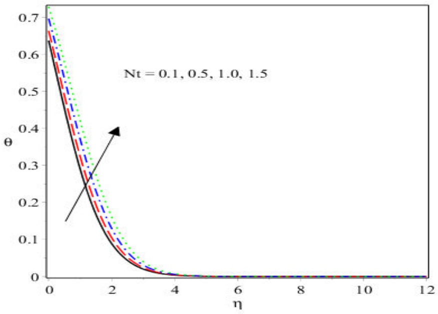

Fig. 9: Effect of *Nt* on temperature.

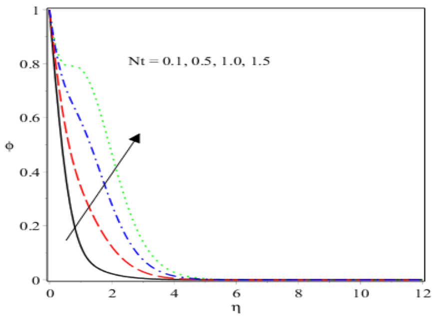

Fig. 10: Effect of *Nt* on concentration.

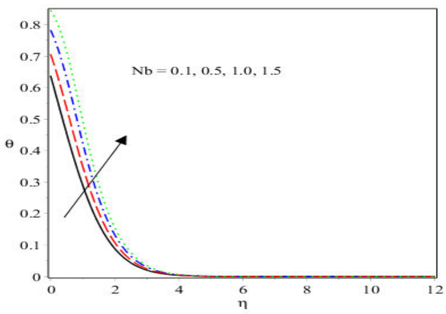

Fig. 11: Effect of *Nb* on temperature

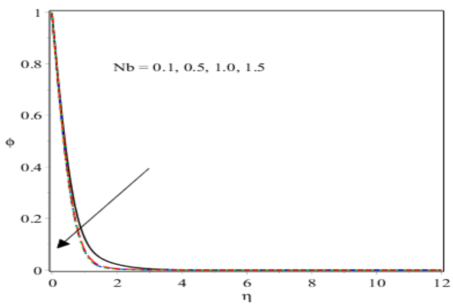

Fig. 12: Effect of *Nb* on concentration.

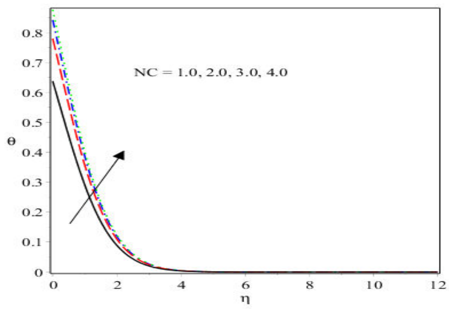

Fig. 13: Effect of *NC* on temperature.

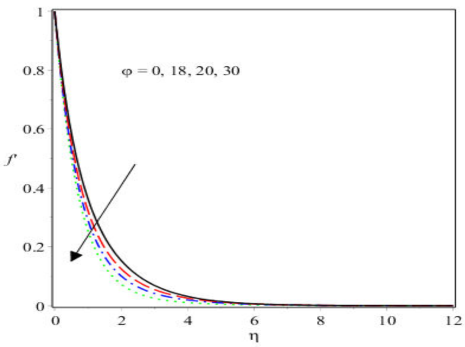

Fig. 14: Effect of plate inclination φ on velocity.

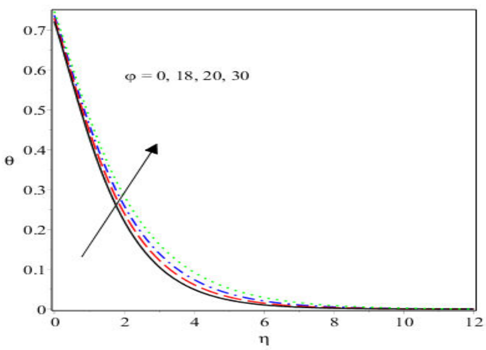

Fig. 15: Effect of plate inclination φ on temperature.

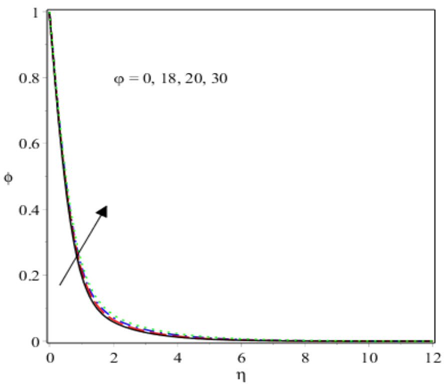

Fig. 16: Effect of φ on concentration.

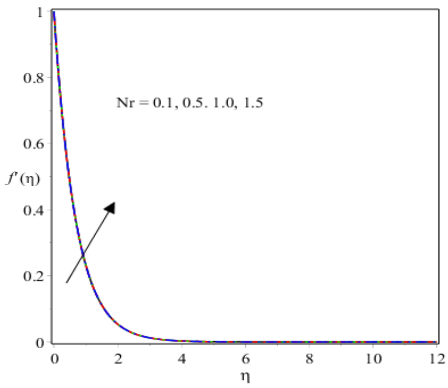

Fig. 17: Effect of *Nr* on velocity.

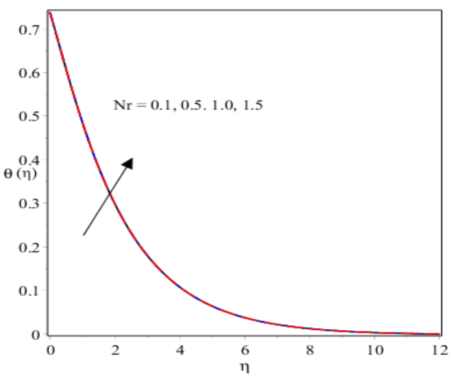

Fig. 18: Effect of *Nr* on Temperature.

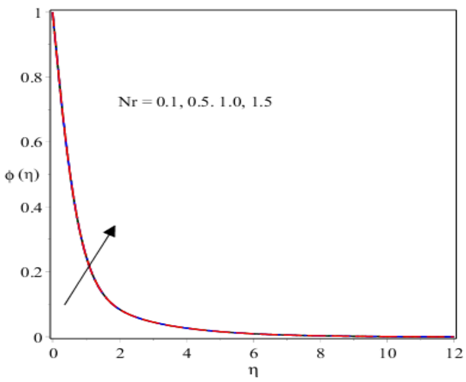

Fig. 19: Effect of *Nr* on concentration.

CONCLUSION:

The following conclusions are interesting drawn from this article. The inclusion of the convective boundary condition, as opposed to the usual continuous heat flux, is a novel idea (see **Fig. 13**). This phenomenon is relevant in heat exchanger systems where fluid flow through a solid surface affects the solid surface's conduction. As the permeability of the plate rises, a decrease in nano-fluid temperature is seen. Convective heating, Brownian motion, and thermophoresis parameters, on the other hand, show the opposite pattern. As magnetic field, permeability, and plate inclination values rise, the nanofluid velocity profile decreases. An increase in the Brownian motion parameter decreases the nanoparticle concentration, but contrasting observations are noticed in the case of the thermophoresis parameter. As the plate inclination increases, nanoparticle temperature and concentration are enhanced, in contrast to the nano-particle velocity. That is the momentum the boundary layer decays. As the magnetic field increases, the thermal and the nanovolume fraction boundary layers grow while the momentum the boundary layer thickness decreases. The Lorentz force, which is created by the magnetic field, slows down fluid motion. Therefore, the heat transmission can be evaluated by the appropriately adjusting M. Cooling devices frequently use this idea. By taking into account various base fluid and nanoparticle combinations, heat and mass transfer rates can be lowered. This idea applies by modifying the heat transfer rates for industries that use inclined plates during production. However, this study focused on steady state nano-fluid flow and the associated parameters of interest. Subsequent studies will expand on this study by examining a time dependent flow of nanofluid over an inclined heated plate with the inclusion of the joule-heating and other considerations.

ACKNOWLEDGEMENT:

We, the authors of this article are immensely grateful to the Editor and Reviewers.

CONFLICTS OF INTEREST:

The authors declare no conflict of interest.

REFERENCES:

1) Akter M, Sarker SPK, and Alam MM. (2023). Magnetohydrodynamics (MHD) effects on heat generation and joule heating with non-uniform surface temperature and natural convection flow over a vertical flat plate, *Int. J. Mat. Math. Sci.*, **5**(2), 09-18. https://doi.org/10.34104/ijmms.023.09018

2) Al-Mamun A, Biswas, P. and Khan, Md. (2019). Computational Modeling on Mhd Radiative Sisko Nanofluids Flow Through A Nonlinearly Stretching Sheet IJHT, **37**, 285-95. https://doi.org/10.18280/ijht.370134
3) Amer, A. M, Al-Rashdi, S. A. S, Ghonem, N. I. and Megahed, A. M. (2023). Tangent Hyperbolic Nanofluid Flowing Over a Stretching Sheet through a Porous Medium with the Inclusion of Magnetohydrodynamic and Slip Impact. *Results In Engineering*, **19**, 101370, https://doi.org/10.1016/j.rineng.2023.101370
4) Ayub,M, Abbas, T. and Bhatti, M.M(2016). Inspiration Of Slip Effects On Electro magneto hydrodynamics(Emhd) Nanofluid Flow Through A Horinzontal Riga Plate. *Eur. Phys. J Plus*, **131**, 193. https://doi.org/10.1140/epjp/i2016-16193-4
5) Aziz, A, Khan, W. A. and Pop, I. (2012). Free Convection Boundary Layer Flow Past A Horizontal Flat Plate Embedded In A Porous Medium Filled By Nanofluid Containing Gytactic Microorganisms. *Inter J. of Thermal Sciences*, **56**, 48-57. https://doi.org/10.1016/j.ijthermalsci.2011.10.001
6) Ahmed, M. S. and Elsaid, A.M (2019). Effect of Hybrid & Single Nanofluids on the Performance Characteristics of Chilled Water Air Conditioning System. *Applied Thermal Engineering,* **163**, 114398. https://doi.org/10.1016/j.heliyon.2023.e18028
7) Alam, Md. S, Islam, Md. R, Ali, and M, Alim. (2015). Magnetohydrodynamic Boundary Layer Flow of Non-Newtonia Fluid and Combined Heat and Mass Transfer about an Inclined Stretching Sheet. *OJAPPS* 05 279-94. https://doi.org/10.4236/ojapps.2015.56029
8) Ali, A, Noreen, A Salem, and Awais, M. (2021). Heat Transfer Analysis of $Cu - Al_2O_3$ Hybrid Nanofluid with Heat Flux and Viscous Dissipation. *J. Therm. Anal Calorim,* **143**, 2367-77. https://doi.org/10.1007/s10973-020-09910-6
9) Alam, M. S, Rahman, M. M and Sattar, M. A. (2009). On The Effectiveness of Viscous Dissipation and Joule Heating on Steady Hydromagnetic Heat and Mass Transfer Flow Over An Inclined Radiate Isothermal Permeable Surface In The Presence of Thermophoresis. *Communications in Nonlinear Science and Numerical Simulation,* **14**, 2132-43. https://doi.org/10.1016/j.cnsns.2008.06.008
10) Ali, F, Khan, I, Samiulhaq and Shafie, S. (2013). Conjugate Effects of Heat And Mass Transfer on Mhd Free Convection Flow Over An Inclined Plate Embedded In A Porous Medium. *D. Abbott, Ed Plos One,* **8** E65223. https://doi.org/10.1143/JPSJ.81.064402
11) Ali, F, Khan, I, Mustapha. N and Shafie, S. (2012).Unsteady Magnetohydrodynamic Oscillatory Flow of Viscoelastic Fluids in a Porous Channel. *J. Phys. Soc. Jpn,* **81**, 064402, https://doi.org/10.1143/JPSJ.81.064402
12) Aziz, A. and Khan, W. A. (2012). Natural Convective Boundary Layer Flow of a Nanofluid past a Convectively Heated Vertical Plate. *Inter J. of Thermal Sciences,* **52**, 83-90, https://doi.org/10.1016/j.ijthermalsci.2011.10.001
13) Aziz, A. (2009). A Similarity Solution for Laminar Thermal Boundary Layer over a Flat Plate with a Convective Surface Boundary Condition. *Communication in Nonlinear Science and Numerical Simulation,* **14**, 1064-8. https://doi.org/10.1016/j.cnsns.2008.05.003
14) Bejan, A. and Bejan A (2013). Convection Heat Transfer. *Wiley Hoboken, Nj,* https://doi.org/10.1007/s00707-004-0155-5
15) Buongiorno, J. (2006). Convective Transport in Nanofluids. *J. of Heat Transfer*, **128**, 240-50, https://doi.org/10.1007/s00707-004-0155-5
16) Chen, C, H. (2004). Heat and Mass Transfer in Mhd Flow By Natural Convection From A Permeable Inclined Surface With Variable Wall Temperature & Concentration. *Acta Mechanica,* **172**, 219-35. https://doi.org/10.1007/s00707-004-0155-5
17) Dhanal, R, Rana, P. and Kumar, L. (2015). Multiple Solution of Mhd Boundary Layer Flow And Heat Behavior Of Nanofluid Induced By A Power-Law Stretching/ Shrinking Permeable Sheet With Viscous Dissipation. *Power Technology*, **273**, 62-70. https://doi.org/10.1016/j.powtec.2014.12.035
18) Goya, M. and Bhargava, R. (2014). Numerical Study of Thermodiffusion Effects on Boundary Layer Flow of Nanofluids over a Power Law Stretching Sheet. *Microfluid Nanofluid*, **17**, 591-604. https://doi.org/10.1007/s13204-013-0254-5
19) Goyal, M. and Bharagava, R. (2014). Boundary Layer Flow and Heat Transfer of Viscoelestic Nanofluids past a Stretching Sheet with Partial Slip Condition. *Appl. Nansci*, **4**, 761-7. https://doi.org/10.1007/s13204-013-0254-5

20) Goyal, M and Bhargava, R. (2018). Simulation of Natural Convective Boundary Layer Flow of a Nanofluid past a Convectively Heated Inclined Plate In The Presence of Magnetic Field. *Int. J. Appl. Comp Math,* **4**, 63. https://doi.org/10.1007/s40819-018-0483-0
21) Ghalambaz, M Noghrehabadi, A. and Ghanbarzadeh, A. (2014). Natural Convection of Nanofluids over a Convectively Heated Ver-tical Plate Embedded in a Porous Medium. *Braz Chem. Eng*, **31**, 413-27. https://doi.org/10.1590/0104-6632.20140312s00001956
22) Gunisetty, M, Reddy, P. B. A and A. D. (2023). Entropy Generation Analysis on Emhd Non-Newtonian Hybrid Nanofluid Flow over a Permeable Rotating Disk through Semi Analytical & Numerical Approaches. Proceedings of the Institute of Mechanical Engineers, Part E. *J. of Process Mechanical Engineering*. https://doi.org/10.1177/09544089231199640
23) Kuznetsov, A.V and Nield, D.A. (2010). Natural Convective Boundary-Layer Flow of a Nanofluid past a Vertical Plate. *Inter J. Of Thermal Sciences*, **49**, 243-7. https://doi.org/10.1016/S0735-1933(03)00196-9
24) Khan, I Ali, F, Shafie, S. and Mustapha, N. (2011). Effects of Hall Current and Mass Transfer on the Unsteady Magnetohydrodynamic Flow in a Porous Channel. *J. Phys. Soc. Jpn,* **80**, 064401. https://doi.org/10.1143/JPSJ.80.064401
25) Mohebbi, N. A. J, Alhajri, E, And Karimi, N. (2020) Analysis Of Transport Process In A Reacting Flow Of Hybrid Nanofluid Around A Bluff-Body Embedded In A Porous Media Using Artificial Neural Network And Particle Swarm Optimization. *J. of Molecular Liquids,* **313**, 113-492. https://doi.org/10.1016/j.molliq.2020.113492
26) Muhamad, H. M. H, Norihan, Md. A, and Safaa, J. A. (2023). Natural Convection in Trapezoidal Cavity Containing Hybrid Nanofluid. *Armne*, **13**, 18-30. https://doi.org/10.37934/armne.13.1.117
27) Narahari, M, Akilu, S and Jaafar, A. (2013). Free Convection Flow of a Nanofluid Past an Isothermal Inclined Plate. *Amm,* **390**, 129-33. https://doi.org/10.4028/www.scientific.net/AMM.390.129
28) Olanrewaju, P. O, Fenuga, O. J, and Okedayo, T.G. (2013). Dufour and Soret Effects on Convection Heat and Mass Transfer in an Electrical Conducting Power Law Flow over a Heated Porous Plate. *Inter J. for Computational Methods in Engineering Science and Mechanics,* **14**, 32-9. https://doi.org/10.1080/15502287.2012.698703
29) Siddiqa, S., Hessain, M, Saha, S.C. (2014).The effect of thermal radiation on the thermal convection boundary layer flow over a wavy horizontal surface. *Int. j. therm. Sci.*, **84**, 142-150. https://doi.org/10.1016/j.ijthermalsci.2014.05.006

Citation: Esekhaigbe E, Uka AU, and Musa A. (2023). Magnetohydrodynamic effects on the flow of nanofluids across a convectively heated inclined plate through a porous medium with a convective boundary layer, *Int. J. Mat. Math. Sci.*, **5**(5), 41-51. https://doi.org/10.34104/ijmms.023.041051